Impact of denaturation with urea on recombinant apolipoprotein A-IMilano ion-exchange adsorption: Equilibrium uptake behavior and protein mass transfer kinetics

ARTICLE *in* BIOTECHNOLOGY JOURNAL · JANUARY 2007

Impact Factor: 3.49 · DOI: 10.1002/biot.200600165 · Source: PubMed

8 AUTHORS, INCLUDING:

Tapan K Das
Bristol-Myers Squibb
79 PUBLICATIONS **1,642** CITATIONS
SEE PROFILE

Sa V Ho
Pfizer Inc.
44 PUBLICATIONS **597** CITATIONS
SEE PROFILE

DOI 10.1002/biot.200600165 Biotechnol. J. 2007, 2, 110–120

Research Article

Impact of denaturation with urea on recombinant apolipoprotein A-I_{Milano} ion-exchange adsorption: Equilibrium uptake behavior and protein mass transfer kinetics

Alan K. Hunter[1], Eric J. Suda[2], Tapan K. Das[1], Robert E. Shell[1], John T. Herberg[1], Natraj Ramasubramanyan[1], Mark E. Gustafson[1] and Sa V. Ho[1]

[1]Pfizer Inc., Global Biologics, Chesterfield, MO, USA
[2]Manpower Professional Inc., Chesterfield, MO, USA

We have studied the equilibrium uptake behavior and mass transfer rate of recombinant apolipoprotein A-I_{Milano} (apo A-I_M) on Q Sepharose HP under non-denaturing, partially denaturing, and fully denaturing conditions. The protein of interest in this study is composed of amphipathic α helices that serve to solubilize and transport lipids. The dual nature of this molecule leads to the formation of micellar-like structures and self association in solution. Under non-denaturing conditions equilibrium uptake is 134 mg/mL media and the isotherm is essentially rectangular. When fully denatured with 6 M urea, the equilibrium binding capacity decreases to 25 mg/mL media and the isotherm becomes less favorable. The decrease in both binding affinity and media capacity when the protein is completely denatured with 6 M urea can be explained by the loss of all alpha helical structure. The rate of apo A-I_M mass transfer on Q Sepharose HP was characterized using a macropore diffusion model. Results of modeling studies indicate that effective pore diffusivity increases from 4.5×10^{-9} cm^2/s in the absence of urea to 6.0×10^{-8} cm^2/s when apo A-I_M is fully denatured with 6 M urea. Based on light-scattering data reported for apo A-I, protein self association appears to be the dominant cause of slow protein mass transfer observed under non-denaturing conditions.

Received 24 August 2006
Revised 18 September 2006
Accepted 21 September 2006

Keywords: Apolipoprotein A-I_{Milano} · Chromatography · Ion exchange · Mass transfer · Self association

1 Introduction

Urea is a frequently used component during bioprocessing and manufacture of recombinant proteins. The chaotropic properties of urea make it useful as a strong denaturant. It has seen broad application for the solubilization and refolding of protein inclusion bodies obtained from *Escherichia coli* (*e.g.*, [1–6]). There have been a smaller number of reports of urea used in conjunction with ion-exchange adsorption. Most examples in the literature in which urea has been utilized during ion-exchange chromatography describe adsorptive refolding processes (*e.g.*, [7–11]), or the purification of crude protein mixtures obtained from solubilized inclusion bodies prior to a conventional refolding step (*e.g.*, [12–14]). Urea has also been used in analytical ion-exchange HPLC biophysical characterization studies (*e.g.*, [15, 16]).

There are several drawbacks to utilizing urea during the manufacture of recombinant proteins. Chief among them are the raw material costs, waste disposal considerations, and chemical modification of the protein of interest resulting in carbamylation. In aqueous solution urea decomposes to form cyanate and ammonium ions [17]. The cyanate is capable of reaction with numerous polypeptide functional groups to yield carbamyl deriva-

Correspondence: Alan K. Hunter, 700 Chesterfield Village Parkway, Chesterfield, MO 63017, USA
E-mail: alan.k.hunter@pfizer.com

Abbreviations: apo A-I_M, apolipoprotein A-I_{Milano}; **CD**, circular dichroism; **CV,** column volume; **DBC**, dynamic binding capacity

tives [18]. The modification of recombinant therapeutic proteins via carbamylation is undesirable for several reasons. Reduced bioactivity has been observed due to protein carbamylation [19]. Furthermore, carbamylated proteins have been reported to be immunogenic in animal models [20].

Apolipoprotein A-I (apo A-I) is a 28-kDa protein present in human plasma in low concentration. Apo A-I is the major protein component of high-density lipoprotein (HDL), which serves to maintain cholesterol homoeostasis and eliminate excess cholesterol [21]. Apolipoprotein A-I_{Milano} (apo A-I_M) is a naturally occurring variant of apo A-I that appears to confer protection against cardiovascular disease to those who carry the mutated gene [22]. The mutation results in an arginine residue at position 173 being substituted with cysteine [23]. The free thiol on the cysteine residue can oxidize to form a disulfide-bonded apo A-I_M homodimer [22]. Both apo A-I and apo A-I_M are composed of amphipathic α helices, leading to self association and the formation of dynamically interacting micellar-like structures in solution [21, 22, 24]. Consistent with micelle formation, the mean hydrodynamic radius of apo A-I, as measured by quasi-elastic light scattering, increases under conditions that favor self association [21]. Conversely, in the presence of a chaotrope the mean hydrodynamic radius of apo A-I decreases [21].

In assessing the performance of ion-exchange adsorbents for the purification of recombinant proteins, an understanding of equilibrium uptake behavior and mass transfer rates is critically important. For bioprocess applications where large diameter adsorbent beads and high mobile phase velocities are typically utilized, chromatographic efficiency is nearly completely determined by mass transfer kinetics [25]. Accordingly, numerous studies have been devoted to protein mass transfer in chromatography media (*e.g.*, [26–31]). However, to our knowledge, the effects of urea on protein-binding capacity, chromatography retention, and intraparticle mass transfer in ion-exchange columns have not been investigated in a systemic fashion. From a practical viewpoint, knowledge of these effects is critical for the selection of suitable stationary phases and of proper operating conditions. The urea concentration is an important design variable that needs to be optimized. Adding too little urea may result in broad peaks and shallow breakthrough curves, particularly if the protein is present in multiple self-associated forms. On the other hand, adding too much urea may lead to denaturation or unfolding of the protein, which in turn, while giving rise to sharp peaks and sharp breakthrough curves, can adversely affect the binding capacity. Thus, an optimum may exist striking a good balance between capacity and chromatographic band broadening.

In this work, using apo A-I_M as a model system, we investigate the effects of urea on binding capacity and mass transfer in anion-exchange chromatography. We first characterize the apo A-I_M denaturation behavior using circular dichroism (CD). Experiments are conducted to determine equilibrium uptake and column breakthrough behavior for non-denatured, partially denatured, and fully denatured protein. Equilibrium uptake and breakthrough studies were performed under nonlinear conditions that are typically encountered during large-scale bioprocessing. Gradient elution of apo A-I_M at different urea concentrations was also evaluated under nonlinear conditions. Mass transfer rates were quantified by fitting breakthrough curves to a model that describes transport in terms of solute diffusion through large open pores within the adsorbent particle. Results of equilibrium uptake experiments and modeling studies are interpreted in light of the unusual physicochemical properties of the apo A-I_M protein.

2 Materials and methods

2.1 Chemicals

Chemicals for the preparation of buffers were obtained from Fisher Scientific (Pittsburgh, PA, USA) and VWR Scientific (West Chester, PA, USA). For use in the preparation of buffers, an 8 M stock urea solution was prepared and purified using mixed bed deionization. The conductivity of the deionized urea was generally less than 5 μS/cm. All buffers were prepared and pH adjusted at room temperature (18–22°C). Buffers were used within 24 h following preparation.

2.2 Recombinant apo A-I_M

The recombinant expression and purification of apo A-I_M has been reported previously [22]. The apo A-I_M protein used for this work was recombinantly expressed using *E. coli*, recovered from the cells, and chromatographically purified. Apo A-I_M forms a homodimer linked via an interchain disulfide bond with a molecular mass of 56 kDa. The purification procedure that was employed resulted in disulfide-bonded dimeric apo A-I_M of high purity.

2.3 Chromatography resin and instrumentation

Q Sepharose HP chromatography resin was obtained from GE Healthcare (Piscataway, NJ, USA) and used for all experiments described in this work. Chromatography experiments were conducted using a GE Healthcare Akta Explorer 100. All adsorption experiments were performed at room temperature and utilized 0.5-cm diameter Tricorn columns obtained from GE Healthcare.

2.4 Equilibrium uptake experiments

Equilibrium uptake experiments were conducted by equilibrating Q Sepharose HP resin in 20 mM Tris, 50 mM

NaCl, pH 7.8 containing 0 M, 2 M, or 6 M urea. The resin was centrifuged and the supernatant decanted to yield a thick slurry. Between 0.1 and 0.2 g resin was carefully weighed and placed in 10 mL glass scintillation vials. Using the same buffers used to equilibrate the resins, 4 mL of solution containing a known protein concentration as determined by UV absorbance at 280 nm using a Varian Cary 50 spectrophotometer (Palo Alto, CA, USA) was added to the vials containing resin. The resin-protein mixtures were gently agitated on a nutator overnight and allowed to come to equilibrium. Resin was removed by centrifugation and the supernatant protein concentration was determined by UV absorbance at 280 nm. The protein concentration in the resin was determined by material balance according to:

$$q' = \frac{V}{M_w}(C_0 - C) \quad (1)$$

where q' is the protein concentration in the resin (mg/g), V is the fluid volume (mL), M_w is the mass of wet resin (g), C_0 is the initial protein concentration (mg/mL), and C is the final fluid phase protein concentration (mg/mL). The concentration based on resin mass was converted to uptake based on packed bed volume q using the static capacity of the resin determined by numerical integration of experimental breakthrough curves as described below.

To convert packed bed volume to media volume, pressure-drop experiments were conducted. To obtain an estimate of the bed void fraction ε_b of laboratory scale Q Sepharose HP columns, pressure-flow curves were fit to the Blake-Kozeny equation [32]:

$$\frac{\Delta P}{L} = 150\frac{\eta u}{\bar{d}_p^2}\frac{(1-\varepsilon_b)^2}{\varepsilon_b^3} \quad (2)$$

where ΔP is the pressure-drop across the packed bed, L is the packed bed length, η is the viscosity, u is the superficial mobile phase velocity, and $\bar{d}_p$ is the average particle diameter (μm). A digital pressure gauge was placed at the column inlet of a 0.5-cm diameter column packed to a depth of 10 cm and the pressure-flow relationship was determined from 0 to 300 cm/h mobile phase velocity in 20 mM Tris, 50 mM NaCl, pH 7.8. The column was then emptied of resin and the system pressure was determined at the same flow rates that were used with the packed column. The viscosity of water at room temperature and an average particle diameter of 34 μm were used in the calculations. The system pressure was subtracted from the column pressure to obtain the pressure-flow relationship for the packed bed alone.

As an independent determination and check of the resin volume used in the isotherm experiments, a known mass of the same moist resin used in the isotherm experiment was resuspended in buffer and packed into a 0.5-cm diameter column. The resulting packed bed volume was used to determine a conversion factor for q from q'. For all experiments, q determined in this fashion was found to be within 15% of that obtained using the static capacity calculated from integration of the breakthrough curve.

2.5 Breakthrough experiments

Breakthrough experiments were conducted using a 0.5-cm diameter column packed to a depth of 10 cm. Purified recombinant apo A-I_M at a concentration of 1.9 mg/mL was applied to the column at 200 cm/h. The mobile phase buffer for breakthrough experiments was 20 mM Tris, 50 mM NaCl, pH 7.8 containing 0 M, 2 M, or 6 M urea. The elution profile was monitored by UV absorbance at 280 nm using the Akta Explorer 100. Following the experiment, the column was taken off-line and the exact UV absorbance of the feed was determined. The UV absorbance of the feed at 280 nm was used to convert the UV absorbance data from the breakthrough curve to C/C_F (where C_F in the bulk fluid protein concentration at column inlet, mg/mL). The static capacity of the packed column was determined by numerical integration of the area above the breakthrough curve using the trapezoid method.

2.6 Gradient elution chromatography

Gradient elution chromatography was conducted using a 0.5-cm diameter column packed to a depth of 20 cm with Q Sepharose HP. For experiments run under non-denaturing conditions, the column was equilibrated with 20 mM Tris, 20 mM NaCl, pH 7.8. Apo A-I_M was applied to the column at 100 cm/h at a concentration of 1 mg/mL in equilibration buffer. The protein was loaded to a concentration of 3 mg/mL packed bed. Following loading, the column was washed with four column volumes (CV) of equilibration buffer. The protein was eluted with a ten-CV linear gradient to 20 mM Tris, 600 mM NaCl, pH 7.8. The elution profile was monitored by UV absorbance at 280 nm using the Akta Explorer 100. For experiments run under denaturing conditions, the same protocol was used except 2 M or 6 M urea was added to the buffers.

2.7 PAGE

SDS-PAGE analysis was performed using standard techniques with an MES buffer and 4–12% Novex NuPAGE Bis-Tris linear gradient acrylamide gels obtained from Invitrogen (Carlsbad, CA, USA). Following electrophoresis, protein was visualized using colloidal CBB G-250 stain obtained from Invitrogen. For SDS-PAGE analysis, 1 μg total protein was loaded per lane.

2.8 Circular dichroism

CD data were collected with a Jasco J-810 spectropolarimeter at a scan speed of 100 nm/min in 190–260-nm range and cell path length of 1.0 cm. CD spectra were corrected for background contribution and CD values were normalized. Apo A-I_M samples for urea denaturation studies were prepared by adding an increasing quantity of buffered urea solution to a series of vials containing fixed amount of protein in 20 mM Tris, 110 mM NaCl, pH 7.8. The samples were incubated overnight at room temperature prior to CD measurements. The final protein concentration of CD samples was approximately 0.1 mg/mL.

3 Results and discussion

3.1 Circular dichroism

Figure 1 shows SDS-PAGE analysis of the purified apo A-I_M protein used for the CD and adsorption studies described in this work. The CD spectrum of apo A-I_M (not shown) suggests predominant helical structure in solution. The unfolding of secondary structure (*i.e.*, helical content) induced by urea was monitored by CD values at 220 nm. The denaturation curve shown in Fig. 2 indicates onset of denaturation at approximately 0.7 M urea. Unfolding is complete by about 4.2 M urea, with a transition midpoint of 2.1 M. A sample prepared in 20 mM Tris, 50 mM NaCl, 6 M urea, pH 7.8, gave a CD value (at 220 nm) of –20.0 mdeg, essentially identical to that obtained in 20 mM Tris, 110 mM NaCl, 6 M urea, pH 7.8.

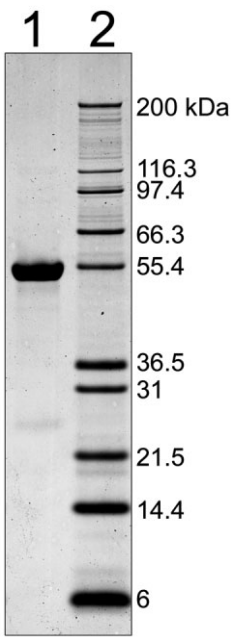

Figure 1. SDS-PAGE analysis of apo A-I_M protein used for CD and adsorption studies. Lane 1 shows 1 µg load of apo A-I_M. Lane 2 shows Invitrogen Mark 12 molecular weight standards.

3.2 Equilibrium uptake experiments

Results of equilibrium uptake experiments are shown in Fig. 3. When no urea is present, the isotherm is very favorable (essentially rectangular) and the maximum capacity is 134 mg/mL media. When the protein is partially denatured with 2 M urea, the isotherm remains rectangular, but the capacity decreases to 85 mg/mL media. In the presence of 6 M urea, equilibrium uptake behavior completely changes. The isotherm becomes less favorable and the maximum capacity decreases to 25 mg/mL media. Solid lines in Fig. 3 represent Langmuir isotherms fitted to the data according to:

$$q = \frac{q_m C}{K_D + C} \tag{3}$$

where q_m is the adsorption capacity and K_D is the dissociation constant. The isotherm parameters, summarized in Table 1, were obtained by linear least squares analysis as previously described [26]. The capacity of the adsorbent was expressed per volume of packed bed and media. Repeated pressure-drop experiments yielded a bed void fraction ε_b value of 0.33 ± 0.01 for 0.5×10 cm Q Sepharose HP packed beds when fit to Eq. (2). This was used as the basis for conversion from packed bed volume to media volume.

To understand the equilibrium uptake behavior of apo A-I_M, it is important to distinguish between the concepts of binding affinity and media capacity. When the protein is partially denatured with 2 M urea, the capacity decreases, but the binding affinity remains very favorable as indicated by the rectangular isotherm. On the other hand, when the protein is completely denatured with 6 M urea both the binding affinity and media capacity decrease. To explain how this behavior arises, we must also distinguish between protein self association and protein fold-

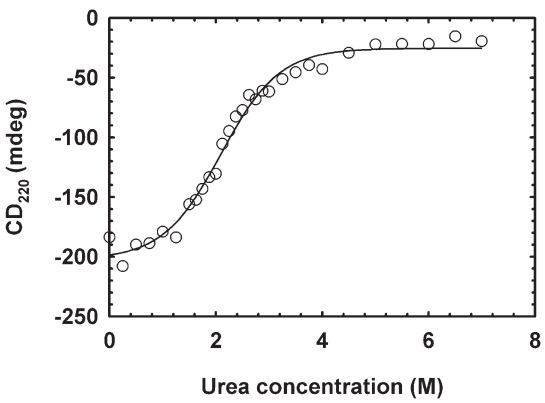

Figure 2. Urea denaturation of apo A-I_M in 20 mM Tris, 110 mM NaCl, pH 7.8. Denaturation curve determined by circular dichroism at 220 nm.

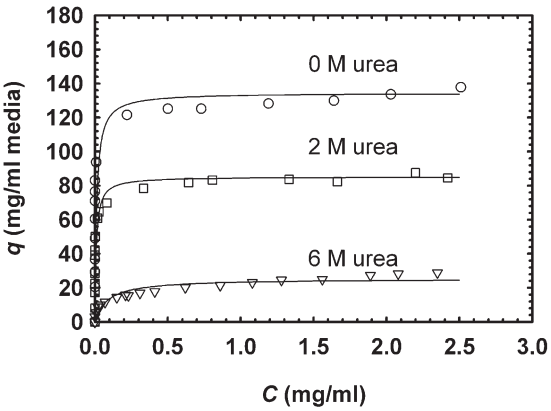

Figure 3. Equilibrium uptake of purified apo A-I_M on Q Sepharose HP in 20 mM Tris, 50 mM NaCl, pH 7.8 containing 0 M, 2 M, or 6 M urea. Solid lines represent fitted Langmuir isotherms according to Eq. (3). Equilibrium parameters are given in Table 1.

ing. Protein self association can result in higher binding capacity as molecules bind not only to the ion-exchange groups in the adsorbent particle, but also to each other. This can be thought of as a form of multilayer adsorption. When protein-protein interactions are modulated using a chaotrope, a decrease in capacity is observed as is seen in the case of the 2M urea isotherm. However, because the protein retains significant α helical structure, binding affinity remains quite favorable. When a protein is folded, hydrophilic and charged residues are typically presented on the surface and interact with the aqueous environment. Secondary and tertiary structure can lead to regions on the protein surface of net negative or positive charge. The characteristics of these charged surface regions and charge distribution can have a dramatic influence on ion-exchange chromatographic behavior [33–35]. Upon complete denaturation with 6 M urea, the protein no longer has a surface in the classic sense and binding of charged residues to the stationary phase may be modulated by the proximity of oppositely charged residues in the primary structure of the protein.

As a protein unfolds, residues are exposed that were previously buried and inaccessible to solvation. As proteins often bury hydrophobic uncharged residues under normal conditions, this can be expected to further reduce binding affinity as these residues will not favorably interact with the adsorbent ion-exchange functional groups. In the case of apo A-I_M, hydrophobic residues may be buried by protein self association, but the effect is similar. Taken together, these effects lead to a decrease in both binding affinity and capacity when the protein is fully denatured, as is shown by the 6 M urea equilibrium uptake isotherm. Obviously, self association and folding are not sequential in nature and there will be overlap between these effects on apo A-I_M equilibrium uptake behavior. From a conceptual standpoint, though, it is useful to separate these phenomena for simplicity and clarity.

Table 1. Langmuir isotherm parameters obtained from fit of experimental equilibrium uptake data shown in Fig. 3

Model parameter	Urea concentration[a)]		
	0 M	2 M	6 M
q_m (mg/mL bed)	90.0	57.1	17.0
q_m (mg/mL media)[b)]	134.4	85.2	25.3
K_D (mg/mL)	0.0118	0.00942	0.0869

a) In 20 mM Tris, 50 mM NaCl, pH 7.8 buffer.
b) Based on ε_b=0.33, from fit of pressure-flow data to Eq. (2).

Accordingly, other proteins would be expected to see a reduction in binding to ion exchangers when denatured with urea. Parente and Wetlaufer [15, 16] observed a large decrease in retention upon urea denaturation for the high performance cation-exchange chromatography of α-chymotrypsinogen-A and lysozyme. Machold *et al*. [36] observed a decrease in binding capacity for α-lactalbumin on Source 30Q under reduced and denatured conditions. In their detailed study, the lower dielectric constant of urea containing solutions was noted as a possible explanation for the reduced binding capacity. This effect may also be a contributing factor in the case of the lower binding capacity observed in our study for apo A-I_M on Q Sepharose HP. The increase in buffer ionic strength due to the formation of cyanate can be ruled out as the cause of lower apo A-I_M binding as the urea utilized for this work was deionized and used within 24 h following preparation. Additionally, build up of cyanate in urea solutions occurs relatively slowly under normal conditions. For example, a 6.7 M urea solution held for 24 h at 25°C contains approximately 0.5 mM cyanate [37].

3.3 Breakthrough behavior

Results of breakthrough experiments are shown in Fig. 4. The breakthrough curves are plotted on the basis of loading per mL packed bed. When the protein is fully denatured with 6 M urea, the static binding capacity is 16.2 mg/mL bed as determined by numerical integration of the breakthrough curve. Additionally, the dynamic binding capacity (DBC = 10% breakthrough) is very close to the static capacity as is indicated by the sharp breakthrough curve. For the case of partially denatured protein in 2 M urea, the breakthrough curve remains quite sharp, with similar static and dynamic capacity. However, the static capacity in 2 M urea increases to 56.8 mg/mL bed. For breakthrough with no urea in the buffer, the DBC remains similar to the 2 M urea case, but the curve becomes broader and the static capacity increases. Numerical integration of the area above the breakthrough curve reveals that the static capacity is 89.5 mg/mL bed. Thus, the DBC under non-denaturing conditions represents only 61% of the static capacity of the resin.

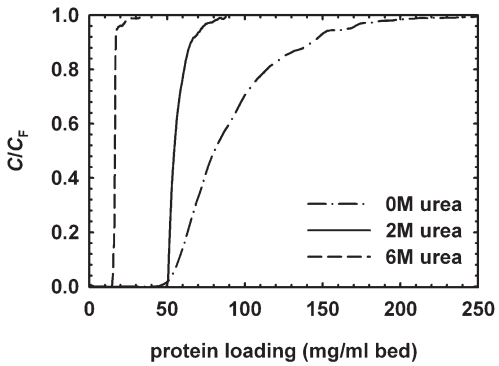

Figure 4. Breakthrough of purified recombinant apo A-I_M on 0.5 × 10 cm Q Sepharose HP packed bed in 20 mM Tris, 50 mM NaCl, pH 7.8 containing 0 M, 2 M, or 6 M urea. Inlet apo A-I_M feed concentration is 1.9 mg/mL and mobile phase velocity is 200 cm/h.

3.4 Gradient elution chromatography

Figure 5 shows gradient elution chromatography of apo A-I_M run with 0 M, 2 M, or 6 M urea in the buffers. When the protein is completely unfolded in 6 M urea, it eluted as a single peak at approximately 120 mM NaCl. In the absence of urea the elution behavior is very different. The protein elutes in a broad tailing peak beginning at approximately 250 mM NaCl and continuing until the end of the gradient at 600 mM NaCl. The peak maximum in the absence of urea was 300 mM NaCl. For the experiment run with 2 M urea, the behavior is intermediate as the elution salt concentration is 220 mM. Interestingly, the elution peak with 2 M urea is sharper than either the 6 M or 0 M urea cases. This could be due to faster mass transport, nonlinear isotherm effects, protein self-association, or combination of these effects.

The elution order of the protein, 6 M < 2 M < 0 M urea, is consistent with the results of equilibrium uptake and

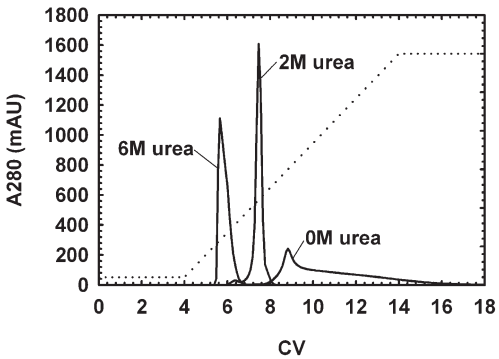

Figure 5. Gradient elution chromatography of purified recombinant apo A-I_M on 0.5 × 20 cm Q Sepharose HP packed bed in 20 mM Tris, pH 7.8 containing 0 M, 2 M, or 6 M urea. Protein loading is 3 mg/mL resin and mobile phase velocity is 100 cm/h. Dotted line shows NaCl gradient on 0–700-mM scale.

breakthrough experiments. The gradient elution experiments also appear to show chromatographic efficiency to be much poorer under non-denaturing conditions as compared to the 2 M and 6 M urea elution curves. This is presumably due to apo A-I_M self association and hindered diffusion effects. In the next section we quantitatively determine the extent to which self association and denaturation impacts protein mass transport kinetics and hindered diffusion.

3.5 Apo A-I_M mass transfer kinetics

As a means to quantitatively assess the impact of denaturation on mass transport kinetics, the apo A-I_M breakthrough curves shown in Fig. 4 were fit to a macropore diffusion model. This is of interest as mass transfer resistance is typically the principal cause of band broadening for the preparative ion-exchange chromatography of proteins [25]. The following equations provide a description of fixed-bed adsorption incorporating external film resistance, axial dispersion, and diffusion in large open pores within the particle [38]:

$$\nu\frac{\partial C}{\partial z}+\frac{\partial C}{\partial t}+\frac{3k_f(1-\varepsilon_b)}{\varepsilon_b r_b}(C-C_{p,r=r_p})=D_L\frac{\partial^2 C}{\partial z^2} \quad (4)$$

$$(1-\varepsilon_p)\frac{\partial q_\pi}{\partial t}+\varepsilon_p\frac{\partial C_\pi}{\partial t}=D_e\left[\frac{1}{r^2}\frac{\partial}{\partial r}\left(r^2\frac{\partial C_\pi}{\partial r}\right)\right] \quad (4a)$$

$$t=0,\ C=0;\ C_p=0 \quad (5)$$

$$z=0,\ \frac{\partial C}{\partial z}=\frac{\nu}{D_L}(C-C_F);\ z=L,\ \frac{\partial C}{\partial z}=0 \quad (5a)$$

$$r=0,\ \frac{\partial C_p}{\partial r}=0;\ r=r_p,\ \frac{\partial C_p}{\partial r}=\frac{k_f}{D_e}(C-C_{p,r=r_p}) \quad (5b)$$

where ν is the mobile phase superficial velocity, cm^2/s, z is the bed length coordinate, k_f is the external film mass transfer coefficent, r_p is the particle radius, r is the particle radial coordinate, C_p is the protein concentration in the pore fluid, D_L is the axial dispersion coefficient, ε_p is the particle porosity, q_p is the absorbed phase concentration in equilibrium with C_p, D_e is the effective pore diffusivity.

In this model, the driving force for mass transfer is the solute concentration gradient in the fluid filling the pores. Eqs. (4) and (5) appropriately describe Sepharose ion-exchangers as they are composed of cross-linked agarose comprising a rigid porous structure [39]. The open porous structure of this material results in protein mass transfer occurring principally by diffusion through the liquid-filled pores [39, 40]. Under strong binding conditions associated with a very favorable equilibrium uptake isotherm, Eqs. (4) and (5) predict a shock transition in the adsorbed

phase protein concentration or "shrinking core" behavior. This phenomenon has been observed at the microscopic level for Sepharose FF cation-exchangers using fluorescently labeled proteins [30, 31].

Eqs. (4) and (5) incorporate a number of parameters that must be independently determined or estimated prior to obtaining a fit for D_e. Bed void fraction ε_b was determined to be 0.33 from pressure-drop experiments as described in the preceding section. The film mass transfer coefficient k_f was estimated using the correlation of Wilson and Geankoplis [41]:

$$Sh = \frac{1.09}{\varepsilon_b} Re^{\frac{1}{3}} Sc^{\frac{1}{3}} \tag{6}$$

where the Sherwood number $Sh=k_f d_p/D$, the Reynolds number $Re=\varepsilon_b v d_p/\nu$, and the Schmidt number $Sc=\nu/D$. The kinematic viscosity values used in the estimates accounted for changes in viscosity and density caused by urea [42]. The mobile phase interstitial velocity was calculated as $v=u/\varepsilon_b$. A value of 600 cm/h was used in the calculations. The free solution diffusivity D is required to calculate the Schmidt number (Sc) in Eq. (6). Due to the self association of apo A-I_M, D is difficult to estimate. An initial value was obtained from the correlation of Polson [26]:

$$D = 9.4\times10^{-15}\frac{T}{\eta M_A^{\frac{1}{3}}} \tag{7}$$

where M_A is the molecular mass, T is the temperature in K.

Changes in viscosity due to urea were also taken into account when calculating free solution diffusivities [42]. To determine if the uncertainty in this estimate impacted the fit of D_e, a sensitivity analysis of k_f was performed as described below.

In general, when combined with a nonlinear isotherm Eqs. (4) and (5) require a numerical solution. However, an analytical solution exists in the irreversible limit, which is satisfied for a Langmuir isotherm when [41]:

$$R = \frac{1}{1+\frac{C_{ref}}{K_D}} < 0.1 \tag{8}$$

where R is the separation factor and C_{ref} is a reference concentration. The feed concentration C_F is normally the reference concentration [25]. When the criterion in Eq. (8) is met, under constant pattern conditions where the number of transfer units (N_{pore}) >2.5+1/Bi [Bi=Biot number (=$k_f r_p/D_e$)], the solution of Eqs. (4) and (5) is well approximated by [43]:

$$(\tau_1-1)N_{pore} = \frac{15}{\sqrt{3}}\tan^{-1}\left(\frac{2\xi+1}{\sqrt{3}}\right) - \frac{15}{2}\left[\ln(1+\xi+\xi^2) - \frac{1}{3}\right] + \frac{5}{Bi}\left[\ln(1-\xi^3)+1\right] - \frac{5\pi}{2\sqrt{3}} \tag{9}$$

$$\tau_1 = \frac{\left(\frac{ut}{L}-\varepsilon_b\right)}{\Lambda} \tag{9a}$$

$$N_{pore} = \frac{15(1-\varepsilon_b)D_e L}{u r_p^2} \tag{9b}$$

$$\xi = \left(1-\frac{C}{C_F}\right)^{\frac{1}{3}} \tag{9c}$$

$$\Lambda = \frac{(1-\varepsilon_b)q_w}{C_F} \tag{9d}$$

$$Bi = \frac{k_f r_p}{D_e} \tag{9e}$$

where τ_1 is the dimensionless time, Λ is the distribution parameter, and q_w is the adsorption capacity.

It should be noted that Eq. (9) does not account for axial dispersion or solute accumulation in the pore fluid; the former is expected to be negligible for this system and the latter is typically unimportant when $q_w \gg C_F$. Using the K_D values shown in Table 1, at C_F=1.9 mg/mL the separation factor $R=6.1\times10^{-3}$, 4.9×10^{-3}, and 4.4×10^{-2} for 0 M, 2 M, and 6 M urea, respectively. Therefore, Eq. (9) was used in modeling studies to describe breakthrough behavior under all three conditions.

Table 2 provides a summary of independently determined or estimated model parameters used to obtain the fit of D_e from the experimental data as is shown in Figs. 6a–c. For each urea concentration, the effective diffusivity was adjusted to provide an approximate fit of the experimental breakthrough curves. Fitted D_e values are summarized in Table 3. As can be seen from the solid lines in the figures, the model accurately captures the salient features of breakthrough behavior and provides a good fit in all cases. As the saturation capacity is approached, the experimental results for all urea concentrations "tail" and diverge slightly from the model. A number of theories have been advanced to explain this phenomenon, which is a common feature of protein breakthrough curves on ion exchangers [25, 44, 45]. Perhaps most interestingly, the fitted effective diffusivity value obtained in the absence of urea $D_e=4.5\times10^{-9}$ cm^2/s was more than an order of magnitude lower than that obtained when the protein was fully denatured with 6 M urea, $D_e=6.0\times10^{-8}$ cm^2/s. When the protein was partially denatured with 2 M urea, the effective diffusivity value obtained from the fit of experimental data was found to be intermediate, $D_e=1.6\times10^{-8}$ cm^2/s. An illustration of how large the differences in mass transfer rates truly are can be seen in Fig. 7. In this figure we use all three fitted D_e values shown in Table 3 with model parameters from Table 2 for 2 M urea and Eq. (9) to simulate breakthrough behavior. Apo A-I_M mass transport rates are higher in the presence of urea despite the fact that urea increases solution viscosity. This effect

Table 2. Summary of independently determined or estimated parameters used to obtain fitted D_e values with Eq. (9). Modeling results shown in Fig. 6. Fitted D_e values shown in Table 3

Model parameter	Urea concentration[a)]		
	0 M	2 M	6 M
u (cm/h)	200	200	200
k_f (cm/s)[b)]	0.0048	0.0045	0.0038
r_p (μm)[c)]	17	17	17
L (cm)	10	10	10
q_w (mg/mL)[d)]	133.6	84.8	24.2
C_F (mg/mL)	1.9	1.9	1.9
ε_b[e)]	0.33	0.33	0.33

a) In 20 mM Tris, 50 mM NaCl, pH 7.8 buffer.
b) Estimated from Eqs. (6) and (7).
c) From manufacturer's literature.
d) From Eq. (3) and equilibrium parameters in Table 1 with C=1.9 mg/mL.
e) From fit of pressure-flow data to Eq. (2).

would tend to lower the rate of protein mass transport if acting alone.

The fit of D_e for apo A-I_M was found to be insensitive to the film mass transfer coefficient k_f. Figures 8a and b show the effect of an order of magnitude change of k_f on simulated breakthrough profiles for 0 M and 6 M urea. The simulated breakthrough curves for both sets of conditions are nearly coincident regardless of the value of k_f. Intraparticle diffusion is the dominant mass transfer resistance for experiments under non-denatured, partially denatured, and fully denatured conditions. Thus, the accuracy of the estimate of k_f using Eqs. (6) and (7) has essentially no impact on the reported D_e values.

Table 3. Summary of D_e values obtained from fit of experimental breakthrough curves with Eq. (9) using model parameters shown in Table 2. Modeling results shown in Fig. 6.

Urea concentration[a)]	D_e (cm²/s)
0 M	4.5×10^{-9}
2 M	1.6×10^{-8}
6 M	6.0×10^{-8}

a) In 20 mM Tris, 50 mM NaCl, pH 7.8 buffer.

The dramatic increase in the rate of mass transfer when apo A-I_M is denatured can be explained as follows. The effective pore diffusivity is related to the free solution diffusivity according to [27]:

$$D_e = \frac{\varepsilon_p}{\tau} D\lambda \tag{10}$$

where τ is the particle tortuosity factor and λ is a hindrance parameter. Porosity and tortuosity are properties of the stationary phase and should remain similar as the ionic strength of the buffers used in breakthrough experiments is essentially equal in all cases. For apo A-I_M in 6 M urea and in the absence of urea it follows that:

$$\frac{D_{e,u}}{D_{e,n}} = \frac{D_u \lambda_u}{D_n \lambda_n} = \frac{6.0 \times 10^{-8}\,\mathrm{cm^2/s}}{4.5 \times 10^{-9}\,\mathrm{cm^2/s}} = 13 \tag{11}$$

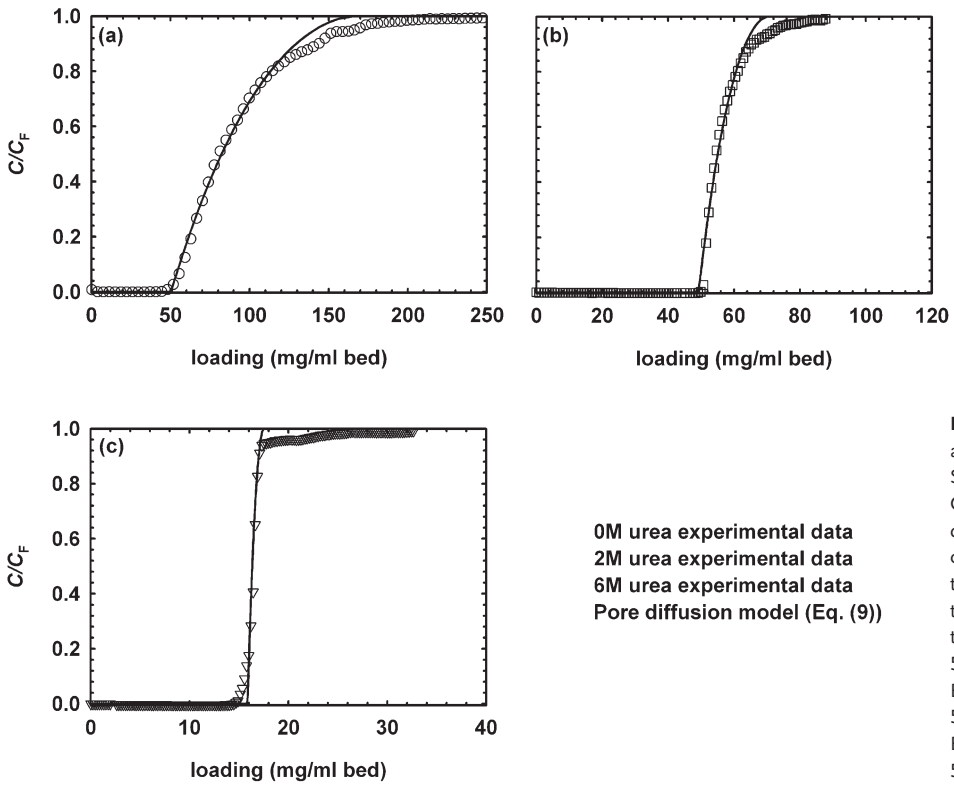

Figure 6. Comparison of experimental apo A-I_M breakthrough curves on Q Sepharose HP with modeling results. Open symbols represent experimental data from UV trace normalized to feed concentration. Solid lines represent solution of Eq. (9) obtained using parameters shown in Tables 2 and 3. (a) Breakthrough of apo A-I_M in 20 mM Tris, 50 mM NaCl, 0 M urea, pH 7.8. (b) Breakthrough of apo A-I_M in 20 mM Tris, 50 mM NaCl, 2 M urea, pH 7.8. (c) Breakthrough of apo A-I_M in 20 mM Tris, 50 mM NaCl, 6 M urea, pH 7.8.

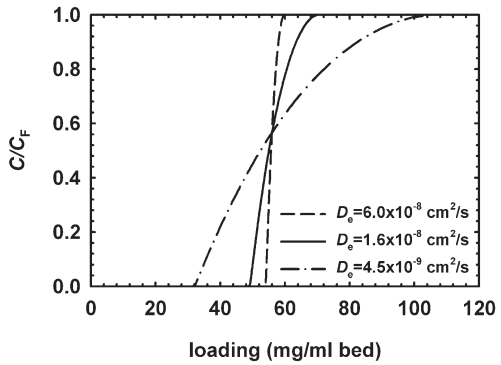

Figure 7. Simulated breakthrough profiles obtained from solution of Eq. (9) using model parameters for 2 M urea from Table 2 and D_e values for 0 M, 2 M, and 6 M urea from Table 3.

where the subscripts u and n denote denatured and non-denatured, respectively. While the free solution diffusivity of apo A-I_M has not been reported, we can obtain an estimate of the ratio D_u/D_n from apo A-I light scattering experiments. At solution concentrations of apo A-I above 1 mg/mL, $D_u/D_n \approx 2$ [21]. It should be noted that guanidine was used as the denaturant in this determination; however, as both urea and guanidine are strong chaotropes, the effect is likely similar. Using $D_u/D_n \approx 2$ as the ratio of free solution diffusivities, $\lambda_u/\lambda_n \approx 6.5$. As apo A-$I_M$ is less self associated than apo A-I at all protein concentrations [22], D_u/D_n is in fact expected to be lower and λ_u/λ_n higher. Therefore, the dominant cause of slow mass transfer under non-denaturing conditions is hindered diffusion.

The increase in hindrance may be caused by a number of factors such as pore blockage or charge repulsion from bound apo A-I_M. However, the most obvious explanation is the amphipathic nature of apo A-I_M and resulting self-associative behavior of the molecule. As apo A-I_M diffuses into a pore, favorable interaction with protein already bound to the pore walls retards movement of the molecule and results in a large decrease in the rate of mass transfer. The larger hydrodynamic radius of self-associated apo A-I_M could also contribute to hindered diffusion. When favorable protein-protein interactions are modulated using urea, the apo A-I_M mass transfer rate into the particle increases. It may be possible to account for the effect of self-association explicitly using a reaction-separation modeling approach [46]. However, the complex nature of apo A-I_M micelle formation may confound such an approach. It remains an open question that is beyond the scope of this work, but certainly worthy of further investigation.

The price for faster mass transfer rates when the protein is partially or fully denatured with urea is lower equilibrium binding capacity. Thus, the goals of an individual ion-exchange unit operation would need to be carefully weighed to determine how to balance these various competing factors. For example, the goal for a capture unit operation is typically maximum binding capacity. On the other hand, maximum resolution and hence minimum protein-protein interaction may be required for difficult separations such as product-related impurities and modified forms.

4 Conclusions

We have studied the equilibrium uptake behavior and protein mass transfer rate of recombinant apo A-I_M on Q Sepharose HP under non-denaturing, partially denaturing, and fully denaturing conditions. Under non-denaturing conditions equilibrium uptake is 134 mg/mL media and the isotherm is essentially rectangular. When the protein is partially denatured with 2 M urea, the shape of the isotherm remains rectangular, but the binding capacity decreases to 85 mg/mL media. When fully denatured with 6 M urea, the equilibrium binding capacity decreases to 25 mg/mL media and the isotherm becomes less favorable. The reduction in media capacity when using 2 M urea can be explained by the modulation of protein-protein interactions. The decrease in both binding affinity and media capacity when the protein is completely denatured with 6 M urea can be explained by the loss of all α helical structure. Folding can lead to regions on the surface of a protein having net negative or positive charge. The characteristics of these charged surface regions and

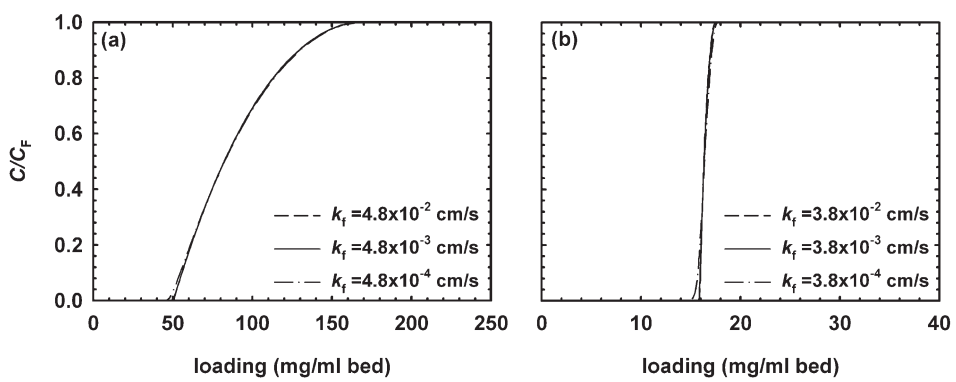

Figure 8. Effect of film mass transfer coefficient k_f on simulated breakthrough profiles from solution of Eq. (9). (a) Simulated profiles obtained using model parameters from Tables 2 and 3 for 0 M urea. (b) Simulated profiles obtained using model parameters from Tables 2 and 3 for 6 M urea.

Nomenclature

Bi	Biot number ($=k_f r_p/D_e$)
C	Bulk fluid protein concentration, mg/ml
C_0	Initial bulk fluid protein concentration, mg/ml
C_F	Bulk fluid protein concentration at column inlet, mg/ml
C_p	Protein concentration in pore fluid, mg/ml
C_{ref}	Reference concentration, mg/ml
d_p	Particle diameter, μm
$\bar{d}_p$	Average particle diameter, μm
D	Free solution diffusivity, cm^2/s
D_e	Effective pore diffusivity, cm^2/s
D_L	Axial dispersion coefficient, cm^2/s
k_f	External film mass transfer coefficient, cm/s
K_D	Dissociation constant, mg/ml
L	Bed length, cm
M_A	Molecular mass, Da
M_w	Mass of resin, g
N_{pore}	Number of transfer units
P	Pressure, Pa
q	Protein concentration in particle, mg/ml
q'	Protein concentration in particle, mg/g
q_m	Adsorption capacity, mg/ml
q_p	Adsorbed phase concentration in equilibrium with C_p, mg/ml
q_w	Adsorption capacity, mg/ml
r	Particle radial coordinate, μm
r_p	Particle radius, μm
Re	Reynolds number ($=\varepsilon_b \nu d_p/\nu$)
Sc	Schmidt number ($=\nu/D$)
Sh	Sherwood number ($=k_f d_p/D$)
t	time, s
T	Temperature, K
u	Mobile phase superficial velocity, cm/s
ν	Mobile phase interstitial velocity, cm/s
V	Volume of solution, ml
z	Bed length coordinate, cm

Greek symbols

ε_b	Bed void fraction
ε_p	Particle porosity
η	Viscosity, cP
λ	Hindrance parameter
Λ	Distribution parameter
ν	Kinematic viscosity, cm^2/s
τ	Tortuosity factor
ξ	Parameter defined by Eq. 9c

charge distribution can have a dramatic influence on chromatographic behavior [33–35]. Upon denaturation, the protein no longer has a surface in the classic sense, and binding of charged residues to the stationary phase may be modulated by the proximity of oppositely charged residues in the primary structure of the protein. Gradient elution experiments also illustrate the change in binding characteristics as the elution salt concentration decreases from 300 mM NaCl in the absence of urea to approximately 120 mM NaCl in 6 M urea. When partially denatured with 2 M urea the elution salt concentration was 220 mM, intermediate of that found in the absence of urea and in 6 M urea. Moreover, in the absence of urea, the apo A-I_M gradient elution peak is very broad and asymmetric. When partially or fully denatured with urea, apo A-I_M elutes in a much sharper and more symmetric peak.

The rate of apo A-I_M mass transfer on Q Sepharose HP was characterized using a macropore diffusion model fit to experimental breakthrough curves. Results of modeling studies indicate that effective pore diffusivity increases from 4.5×10^{-9} cm^2/s in the absence of urea to 6.0×10^{-8} cm^2/s when apo A-I_M is fully denatured with 6 M urea. When partially denatured in 2 M urea, the effective pore diffusivity was found to be intermediate, 1.6×10^{-8} cm^2/s. Based on light scattering data reported for apo A-I [21], protein self association appears to be the dominant cause of slow protein mass transfer observed under non-denaturing conditions. As apo A-I_M diffuses into a pore, favorable interaction with protein already bound to the pore walls retards the movement of the molecule and results in a substantial decrease in the rate of mass transfer. The larger hydrodynamic radius of self-associated apo A-I_M could also be a contributing factor to slow mass transfer. When the favorable protein-protein interactions are modulated using urea, the apo A-I_M mass transfer rate into the particle increases. From a practical viewpoint, our studies suggest that an optimum denaturant concentration likely exists where a good compromise is found between capacity and band broadening. The modeling tools applied in his work allows one to determine the impact of these different effects on process performance providing a rational means for optimization.

We would like to thank the Pfizer Global Biologics process development analytical group and fermentation group for providing support for this work.

5 References

[1] Hart, R. A., Lester, P. M., Reifsnyder. D. H., Ogez, J. R., Builder S. E., Large scale, *in situ* isolation of periplasmic IGF-I from *E. coli*. *Bio/Technology* 1994, *12*, 1113–1117.

[2] Guise, A. G., West, S. M., Chaudhuri, J. B., Protein folding *in vivo* and renaturation of recombinant proteins from inclusions bodies. *Mol. Biotechnol.* 1996, *6*, 53–64.

[3] Lilie, H., Schwarz, E., Rudolph, R., Advances in refolding of proteins produced in *E. coli*. *Curr. Opin. Biotechnol.* 1998, *9*, 497–501.

[4] Misawa, S., Kumagai, I., Refolding therapeutic proteins produced in *Escherichia coli* as inclusion bodies. *Biopolymers (Peptide Science)* 1999, *51*, 297–307.

[5] Middelberg, A. P. J., Preparative protein refolding. *Trends Biotechnol.* 2002, *20*, 437–443.

[6] Tsumoto, T., Ejima, D., Kumagai, I., Arakawa, T., Practical considerations in refolding proteins from inclusion bodies. *Protein Expr. Purif.* 2003, *28*, 1–8.

[7] Suttnar, J., Dyr, J. E., Hamsikova, E., Novak, J., Vonka, V., Procedure for refolding and purification of recombinant proteins from *Escherichia coli* inclusion bodies using a strong anion exchanger. *J. Chromatogr. B* 1994, *656*, 123–126.

[8] Li, M., Zhang, G., Su, Z., Dual gradient ion-exchange chromatography improved refolding yield of lysozyme. *J. Chromatogr. A* 2002, *959*, 113–120.

[9] Li, M., Poliakov, A., Danielson, U. H., Su, Z., Janson, J. -C., Refolding of a recombinant full-length non-structural (NS3) protein from hepatitis C virus by chromatographic procedures. *Biotechnol. Lett.* 2003, *25*, 1729–1734.

[10] Kweon, D.-H., Lee, D.-H., Han, N.-S., Seo, J.-H., Solid-phase refolding of cyclodextrin glycosyltransferase adsorbed on cation-exchange resin. *Biotechnol. Prog.* 2004, *20*, 277–283.

[11] Langenhof, M., Leong, S. S. J., Pattenden, L. K., Middelberg, A. P. J., Controlled oxidative protein refolding using an ion-exchange column. *J. Chromatogr. A* 2005, *1069*, 196–201.

[12] Lai, W. B., Middelberg, A. P. J., The production of human papillomavirus type 16 L1 vaccine product from *Escherichia coli* inclusion bodies. *Bioprocess Biosyst. Eng.* 2002, *25*, 121–128.

[13] Karmodiya, K., Srivastav, R. K., Surolia, N., Production and purification of refolded recombinant *Plasmodium falciparum* β-ketoacyl-ACP reductase from inclusion bodies. *Protein Expr. Purif.* 2005, *42*, 131–136.

[14] Qiang-ming, S., Hong-chao, J., Wei-ming, X., Xin, L., Chang-bai, D., Mao-sheng, S., High-level expression and purification of recombinant huGM-CSF (9-127)/IL-6 (29-184) fusion protein in *Escherichia coli*. *Protein Expr. Purif.* 2005, *42*, 278–285.

[15] Parente, E. S., Wetlaufer, D. B., Influence of urea on the high-performance cation-exchange chromatography of hen egg white lysozyme. *J. Chromatogr.* 1984, *288*, 389–398.

[16] Parente, E. S., Wetlaufer, D. B., Effects of urea-thermal denaturation on the high-performance cation-exchange chromatography of α-chymotrypsinogen-A. *J. Chromatogr.* 1984, *314*, 337–347.

[17] Lin, M.-F., Williams, C., Murray, M. V., Conn, G., Ropp, P. A., Ion chromatographic quantification of cyanate in urea solutions: estimation of the efficiency of cyanate scavengers for use in recombinant protein manufacturing. *J. Chromatogr. B* 2004, *803*, 353–362.

[18] Stark, G. R., Modification of proteins with cyanate. *Methods Enzymol.* 1967, *11*, 590–594.

[19] Stark, G. R., Stein, W. H., Moore, S., Reactions of the cyanate present in aqueous urea with amino acids and proteins. *J. Biol. Chem.* 1960, *235,* 3177–3181.

[20] Steinbrecher, U. P., Fisher, M., Witztum, J. L, Curtiss, L. K., Immunogeniticy of homologous low density lipoprotein after methylation, ethylation, acetylation, or carbamylation: generation of antibodies specific for derivatized lysine. *J. Lipid Res.* 1984, *25*, 1109–1116.

[21] Donovan, J. M., Benedek, G. B., Carey, M. C., Self-association of human apolipoproteins A-I and A-II and interactions of apolipoprotein A-I with bile salts: quasi-elastic light scattering studies. *Biochemistry* 1987, *26*, 8116–8125.

[22] Calabresi, L., Vecchio, G., Longhi, R., Gianazza, E. *et al.*, Molecular characterization of native and recombinant apolipoprotein A-I_{Milano} dimer. *J. Biol. Chem.* 1994, *269*, 32168–32174.

[23] Suurkuusk, M., Hallen, D., Apolipoprotein A-I_{Milano} unfolds via an intermediate state as studied by differential scanning calorimetry and circular dichrosim. *Eur. J. Biochem.* 1999, *264*, 183–190.

[24] Vitello, L. B., Scanu, A. M., Studies on human serum high density lipoproteins. *J. Biol. Chem.* 1976, *251*, 1131–1136.

[25] Carta, G., Ubiera, A. R., Pabst, T. M., Protein mass transfer kinetics in ion exchange media: measurements and interpretations. *Chem. Eng. Technol.* 2005, *28*, 1252–1264.

[26] Skidmore, G. L., Horstmann, B. J., Chase, H. A., Modelling single-component protein adsorption to the cation exchanger S Sepharose FF. *J. Chromatogr.* 1990, *498*, 113–128.

[27] Frey, D. D., Schweinheim, E., Horvath, C., Effect of intraparticle convection on the chromatography of biomacromolecules. *Biotechnol. Prog.* 1993, *9*, 273–284.

[28] Yoshida, H., Yoshikawa, M., Kataoka, T., Parallel transport of BSA by surface and pore diffusion in strongly basic chitosan. *AIChE J.* 1994, *40*, 2034–2044.

[29] Lewus, R. K., Altan, F. H., Carta, G., Protein adsorption and desorption on gel-filled rigid particles for ion exchange. *Ind. Eng. Chem. Res.* 1998, *37*, 1079–1087.

[30] Hubbuch, J., Linden, T., Knieps, E., Ljunglof, A. *et al.*, Mechanism and kinetics of protein transport in chromatographic media studied by confocal laser scanning microscopy. Part I. The interplay of sorbent structure and fluid phase conditions. *J. Chromatogr. A* 2003, *1021*, 93–104.

[31] Dziennik, S. R., Belcher, E. B., Barker, G. A., Lenhoff, A. M., Effects of ionic strength on lysozyme uptake rates in cation exchangers. I: uptake in SP Sepharose FF. *Biotech. Bioeng.* 2005, *91*, 139–153.

[32] Bird, R. B., Stewart, W. E., Lightfoot, E. N., *Transport Phenomena*. Wiley, New York 1960, p. 199.

[33] Yao, Y., Lenhoff, A. M., Electrostatic contributions to protein retention in ion-exchange chromatography. 1. Cytochrome *c* variants. *Anal. Chem.* 2004, *76*, 6743–6752.

[34] Yao, Y., Lenhoff, A. M., Electrostatic contributions to protein retention in ion-exchange chromatography. 2. Proteins with various degrees of structural differences. *Anal. Chem*. 2005, *77*, 2157–2165.

[35] Ladiwala, A., Rege, K., Breneman, C. M., Cramer, S. M., *A priori* prediction of adsorption isotherm parameters and chromatographic behavior in ion-exchange systems. *Proc. Natl. Acad. Sci. USA* 2005, *102*, 11710–11715.

[36] Machold, C., Schlegl, R., Buchinger, W., Jungbauer, A., Martix assisted refolding of proteins by ion exchange chromatography. *J. Biotechnol.* 2005, *117*, 83–97.

[37] Marier, J. R., Rose, D., Determination of cyanate, and a study of its accumulation in aqueous solutions of urea. *Anal. Biochem*. 1964, *7*, 304–314.

[38] Gu, T., *Mathematical Modeling and Scale-up of Liquid Chromatography.* Springer-Verlag, Berlin 1995, pp. 9–22.

[39] Martin, C., Iberer, G., Ubiera, A., Carta, G., Two-component protein adsorption kinetics in porous ion exchange media. *J. Chromatogr. A* 2005, *1079*, 105–115.

[40] Ubiera, A. R., Carta, G., Radiotracer measurements of protein mass transfer: Kinetics in ion exchange media. *Biotechnol. J.* 2006, *1*, 665–674.

[41] LeVan, M. D., Carta, G., Yon, C. M., Adsorption and ion exchange. In: Green, D. W. (Ed.), *Perry's Chemical Engineers' Handbook,* 7th edn. McGraw-Hill, New York 1997, Section 16.

[42] Kawahara, K, Tanford, C., Viscosity and density of aqueous solutions of urea and guanidine hydrochloride. *J. Biol. Chem.* 1966, *241*, 3228–3232.

[43] Weber, T. W., Chakravorti, R. K., Pore and solid diffusion models for fixed-bed adsorbers. *AIChE J.* 1974, *20,* 228–237.

[44] Jin, X., Talbot, J., Wang, N.-H. L., Analysis of steric hindrance effects on adsorption kinetics and equilibria. *AIChE J.* 1994, *40*, 1685–1696.

[45] Hunter, A. K., Carta, G., Effects of bovine serum albumin heterogeneity on frontal analysis with anion-exchange media. *J. Chromatogr. A* 2001, *937*, 13–19.

[46] Whitley, R. D., Van Cott, K. E., Berninger, J. A., Wang, N.-H. L., Effects of protein aggregation in isocratic nonlinear chromatography. *AIChE J.* 1991, *37*, 555–568.